Aging effects on the transport properties in conducting polymer polypyrrole

B. Sixou
Commissariat à l'Energie Atomique/Département de Recherche Fondamentale sur la Matière Condensée/Service d'Etudes des Systèmes et Architectures Moléculaires/Physique des Métaux Synthétiques, 17 rue des Martyrs, 38054 Grenoble Cedex 9, France

N. Mermilliod
Commissariat à l'Energie Atomique/Département d'Etude des Matériaux/Service deGénie des Surfaces et Applications, 17 rue des Martyrs, 38054 Grenoble Cedex 9, France

J. P. Travers
Commissariat à l'Energie Atomique/Département de Recherche Fondamentale sur la Matiere Condensée/Service d'Etudes des Systèmes et Architectures Moléculaires/Physique des Métaux Synthétiques, 17 rue des Martyrs, 38054 Grenoble Cedex 9, France

(Received 26 June 1995)

We present electronic transport studies of the aging process in naphtalene–sulfonate-doped polypyrrole. They include *in situ* conductivity measurements as a function of the aging time up to 1 month, and conductivity and thermoelectric power measurements in the temperature range 300–15 K for different aging times at 120 °C in room atmosphere. We show that while the short-aging-time decay of the conductivity may be accounted for by a law of the type $\sigma_0-\sigma(t_a)\propto\sqrt{t_a}$, the long-aging-time evolution is well described by a stretched exponential, $\sigma=\sigma_0\exp[-(t_a/\tau)^{1/2}]$. Moreover, two distinct temperature dependences have been identified: (i) $\sigma=\sigma_0\exp[-(T_0/T)^{1/2}]$ for aged samples and (ii) $\sigma=\sigma_0\exp[-T_1/T+T_0]$ for as-synthesized or lightly aged samples. The thermal variation of the thermoelectric power can be described by the following law: $S(T)=AT+B+C/T$, where the relative weight of the linear term, A, appears to be a decreasing function of the aging time. All the results are comprehensively explained in terms of conducting grains separated by insulating barriers in which the conduction is controlled by a hopping process of the charge carriers between the grains. The aging phenomenon is found to consist of a decrease of the grain size, in parallel with a broadening of the barriers, as in a corrosion process. As the aging time increases, the size of the conducting grains decreases and then goes below a critical value that is responsible for a crossover in the transport mechanism and therefore in the time dependence of the conductivity as experimentally observed. In the aged samples, this model leads to the existence of a single expression that accounts for both the temperature and the aging-time dependences of the conductivity, i.e., $\ln\sigma(t_a,T)\propto-(t_a/T)^{1/2}$.

I. INTRODUCTION

In the past decade, electronic conducting polymers have attracted extensive interest in both fundamental and applied research. Some technological applications developed at present use among others the transport properties of these materials. But, till now, there has been no widespread agreement on the relevant models used to describe the prevailing conduction mechanism. On the one hand, very ordered structures like highly oriented and stretched polyacetylene or polyaniline exhibit a negative temperature coefficient and very high conductivities ($\sigma>10^2$ S/cm and up to 10^5 S/cm).[1,2] On the other hand, in most polypyrroles, polythiophenes, and polyanilines, the conductivity is lower than 100 S/cm and its temperature dependence generally follows the typical law

$$\sigma=\sigma_0\exp\left[-\left(\frac{T_0}{T}\right)^{\alpha}\right].$$

Such behavior is characteristic of strongly disordered systems in which conduction proceeds through hopping. However, different models lead to such a functional dependence, while they are based on rather different microscopic pictures of the material. Nevertheless, the value of α is considered to provide some information about the conduction mechanism and it is the first criterion to discriminate among the models. The use of the three-dimensional variable-range-hopping model proposed by Mott[3] with $\alpha=\frac{1}{4}$ is in keeping with a long tradition. For the case $\alpha=\frac{1}{2}$, the most commonly invoked descriptions are either hopping with a Coulomb gap,[4] or quasi-one-dimensional (1D) variable-range hopping,[5] or charging-energy-limited tunneling and related models.[6–8] But at present, the issue remains open and the understanding of the relative influence on macroscopic properties of the 1D structure and of the disorder, which is present at every scale of the structure (defects on the chains, heterogeneities in the doping distribution), is far from being complete. Moreover, several works have been devoted to the theoretical search of other microscopic pictures leading to intermediate exponents.[9] Such a great variety of theoretical approaches reflects the wide range of phenomena involved in electronically conducting polymers. Actually, the transport process may differ from one polymer to another, as well as from one sample to another, according to the preparation method.

The wide range of applications of conducting polymers, including antistatic agents, conducting coatings, energy storage, or nonlinear optics, would greatly benefit from a deeper understanding of the transport mechanisms and of their evolution with time, since successful devices require long-term stability. Among the different materials, polypyrrole, doped with various dopants, shows a greater stability as compared to polyacetylene but at the present time, the conduction properties are still limited by structural and chemical disorder.

The continuous and irreversible conductivity degradation observed during thermal aging experiments has been extensively investigated.[10–15] The common feature of these studies is that the key factor explaining the conductivity decrease is supposed to be a degradation reaction which would be limited by oxygen diffusion or described by a first-order kinetics. These approaches can explain some of the observed data but they fail to represent the conductivity changes on large time scales and at elevated aging temperatures. In fact, all those descriptions do not rely on a deep and complete understanding of the underlying microscopic processes but they are based upon the assumption that the conductivity is somehow linearly related to the defect concentration that increases with chemical or structural disorder. In the light of the present knowledge on the electronic properties of conducting polymers, such a hypothesis appears as very oversimplified. As previously reported, the electronic transport is generally governed by hopping, which leads to a more complicated dependence.

Thus, in order to discriminate among the various models, and specify the appropriate picture standing for our samples of polypyrrole, we took advantage of aging experiments which allow a controlled introduction of defects. *In situ* conductivity measurements both as a function of time for several aging temperatures and as a function of temperature for different aging times were combined. Special attention was paid to the effects of long aging times. We have also studied the evolution of the temperature dependence of the thermoelectric power as a function of aging. We show here that it is essential to take all these dependences into account to achieve a rather complete understanding of both the conduction process and the aging phenomenon and to determine which parameters control the transport properties decrease.

In particular, we demonstrate the existence of two limiting transport processes corresponding to long and short aging times and a continuous change from one to the other with aging and, thus, with the increasing structural disorder. The data can be interpreted in terms of conducting grains separated by insulating barriers. We show that such an unusual picture in which the conduction is controlled by charge carrier hopping between the grains succeeds in explaining all the results by means of only one adjustable parameter, namely, the grain size d, and to reconcile old[10–15] and more recent experimental data.[16] It appears that aging results in a decrease of d, as in a corrosion process, in such a way that, with increasing time, it becomes smaller than a critical value which is responsible for a change in the conduction mechanism and therefore for the existence of short- and long-aging-time behaviors of the material.

This paper is organized as follows. After experimental details about the samples in Sec. II, the data we have obtained for the time dependence of σ, the temperature dependence of σ, and the temperature dependence of thermopower are reported and analyzed in Secs. III to V, respectively. As two different behaviors emerge for the transport properties according to the aging time, the discussion of the results as well as their interpretation in the framework of the conducting grain picture are presented in Sec. VI in two separate parts, i.e., VI A, short aging times and VI B, long aging times.

II. SAMPLE PREPARATION

The samples used for this study were either polypyrrole coatings on various textiles (polyester, glass fibers, Kevlar), or polypyrrole powder pressed in the form of pellets, or even electrochemically synthesized polypyrrole films. The powder and film synthesis using standard preparation methods are detailed in Ref. 10. With regard to the polypyrrole coatings, they were synthesized following a one-step or a two-step procedure. In the one-step synthesis, after a cleaning treatment, the fabric is immersed in a polymerization solution (0.1 M $FeCl_3$+4.3×10^{-2} M pyrrole) at 5–7 °C for 6 h without agitation. The fabric was then rinsed with water and dried with warm air. In the two-step synthesis, the fabric was impregnated with a 0.6-M pyrrole solution in ethanol and then immersed in a 2.4-M $FeCl_3$ aqueous solution for 15 min at ambient temperature under soft agitation. The dopants have always been chosen among those ensuring the best conductivities and stabilities such as toluene sulfonate, naphtalene sulfonate, or hydroxy-benzene-sulfonate. The molar ratio of dopant/pyrrole was equal to 0.3.

We have found exactly the same functional dependence of the conductivity with the aging time in all those samples, with of course numerical factors depending on the sample. Our findings appear to be independent of either the type of the synthesis or the nature of the dopant, or even of the physical form of the dopant. Therefore, we here focus on a chemically synthesized polypyrrole (PPY) deposited on a polyester fabric, and doped with naphtalene-2 sulfonate (ANS2). The thickness of the polypyrrole coating was in the range 1–3 μm. The analytical formula as determined by ESCA and chemical analysis was (C_4H_3N), $(C_{10}H_7SO_3^{1-})_{0.28}$, $(FeCl_4^{1-})_{0.02}$, $(H_2O)_{0.5}$, Cl_ε^{1-}, $(SO_4^{2-})_\varepsilon$.

III. CONDUCTIVITY VERSUS AGING TIME

The aging experiments were performed in a thermally regulated chamber at temperatures T_a=140, 120, 100, and 80 °C for durations up to 1 month. The samples were exposed to room atmosphere, which means that we are dealing with an aging process in the presence of both oxygen and water vapor. The conductivity change was continuously monitored, *in situ*, by conventional four-contact methods. The raw data are reported in Fig. 1 where the sample resistance is plotted versus the aging time t_a, in linear scales. The relative decrease of the conductivity $\Delta\sigma/\sigma$ is presented in Fig. 2 as a function of the square root of the aging time. Our data are very similar to results already reported. Such a decay is often accounted for by diffusion-controlled kinetics.[10–14] In such models, $\Delta\sigma$ is supposed to be proportional to the amount of oxygen absorbed and to the density of conductive paths disrupted by the attachment of oxygen at-

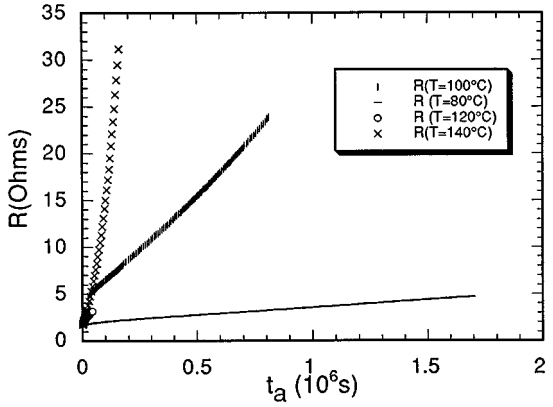

FIG. 1. Resistance of PPY-ANS2 samples as a function of the aging time for various aging temperatures T_a=80, 100, 120, 140 °C.

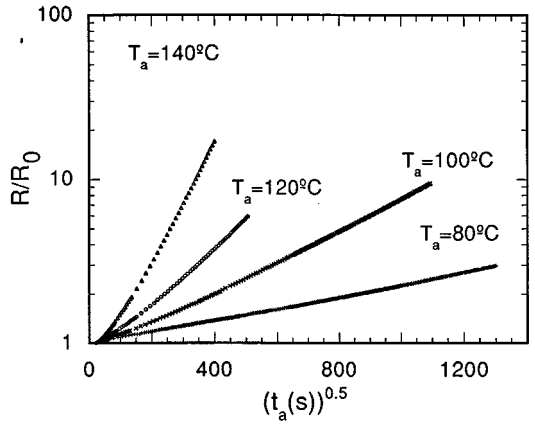

FIG. 3. Logarithmic plot of the resistance of PPY-ANS2 samples as a function of the square root of the aging time for various aging temperatures T_a=80, 100, 120, 140 °C.

oms. The relative decrease of the conductivity is thus expected to vary as $t^{1/2}$. As shown in Fig. 2, this kinetic law gives a rather good description at the very beginning of the thermal treatment where it leads to a straight line. It lasts during time scales significantly longer at low aging temperatures. Experimentally, it gives a correct description when $\Delta\sigma/\sigma \leqslant 1$. But thereafter, we observed deviation from linearity between $\Delta\sigma/\sigma$ and $\sqrt{t_a}$. When the relative variation of the conductivity increases, we observe a transition to another regime with an intermediate quasilinear dependence of σ with t_a.

Alternatively, Samuelson and Druy[15] observed that this decay is apparently a linear function of the aging time t_a for the early stage of the decrease and suggested that the conductivity decay obeys a first-order kinetics. None of these different hypotheses can account for the long time evolution, which our study particularly emphasizes.

The striking result is that, as can be seen in Fig. 3, the evolution of σ can be described in a better way by a stretched exponential of the aging time t_a, for t_a>40 h,

$$\sigma = \sigma_0 \exp(-\sqrt{t_a/\tau}), \tag{1}$$

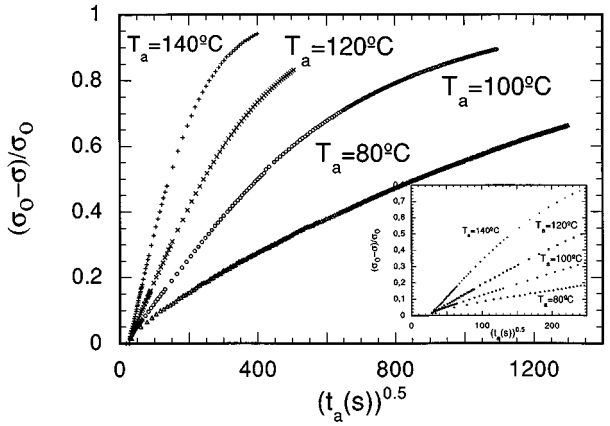

FIG. 2. Relative decrease of the conductivity for PPY-ANS2 samples versus $\sqrt{t_a}$ for the aging temperatures T_a=80, 100, 120, 140 °C.

where τ is the characteristic time of the degradation process (at 120 °C, τ=17 h). The same type of functional dependence has been observed in polyalkylthiophenes.[17] Comparing the evolution at 140, 120, 100, and 80 °C, it appears that τ follows an Arrhenius law as a function of the aging temperature with an activation energy of the order of 1 eV. Since all the $\sigma(t_a)$ curves show the same functional dependence, the evolution of the conductivity at 120 °C can be considered as fully representative of the aging phenomena. Then, in the following, we will concentrate on aging experiments performed at 120 °C. Looking carefully, the kinetic regime described by Eq. (1) is only valid for long thermal treatment times (t_a>40 h) as shown in Fig. 4. Such a complex kinetic law means that the conductivity can hardly be related to the defects concentration in a simple way, in contradiction to what is usually proposed.

IV. CONDUCTIVITY VERSUS TEMPERATURE

We now detail the temperature dependence of the conductivity of the PPY-ANS2 samples after aging at 120 °C for various durations from 0 to 1 month, given in Table I. After aging in room atmosphere, the samples were stored at room temperature in inert argon atmosphere in order to prevent further aging before measurements. A conventional four-probe method was applied. Samples of typical size 8×5×0.5

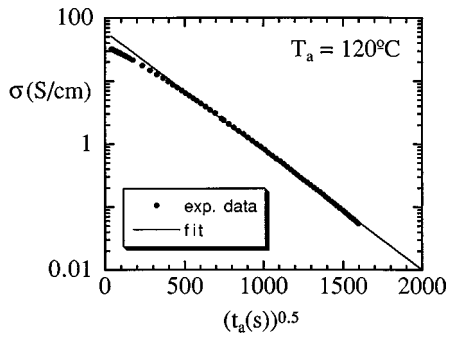

FIG. 4. Conductivity of a PPY-ANS2 sample, as a function of the time t_a, during thermal treatment at 120 °C: dots, experimental data; solid line, best fit obtained with Eq. (1).

TABLE I. Aging times for each sample.

PPY sample	$T0$	$T5$	$T6$	$T7$	$T8$	$T9$	$T10$	$T11$	$T12$
Aging time ($\times 10^4$ s)		2.2	6.25	10.8	17.3	60.5	104	170	233

mm^3 were mechanically pressed on four parallel gold wires. The dc current was provided by a Keithley 220 current source and two Keithley 617 programmable electrometers with an input impedance of $10^{14}\ \Omega$ were used to measure the voltage drop between the inner contacts. The linearity of the voltage versus current characteristics was systematically checked on a one order of magnitude current range. Possible thermoelectric effects were excluded by measurements in both current senses.

The low-temperature measurements were performed in an Oxford Instrument cryostat in the range 15–300 K. The measuring cell was placed in a closed chamber filled with low-pressure He as an exchange gas. The maximum average power dissipated in the sample from the generator was 5 μW. The temperature of the cryostat was controlled and regulated using a computer-driven Oxford temperature controller ITC4. The sample temperature was measured using a calibrated platinum resistor in the range 300–40 K or a calibrated carbon glass resistor in the range 40–15 K.

It must be emphasized that none of our samples displayed a metallic behavior. Consequently, we are here concerned with the effect of aging on originally disordered materials, contrary to the case that was considered by Ishiguro *et al.*[18] or by Reghu and co-workers.[1–2] The thermal variations of the conductivity are presented for the whole set of samples in Fig. 5. For each sample, the $\sigma(T)$ data were fitted to

$$\sigma=\sigma_0\exp\left[-\left(\frac{T_0}{T}\right)^{\alpha}\right], \tag{2A}$$

with σ_0 a constant. In general, the best fit was achieved for $\alpha=0.5$, as observed in Fig. 5, except for the samples with aging times shorter than seven hours ($T0,\ldots,T6$). Therefore, for long aging times (samples $T7$ to $T12$), the conductivity is well described by the following law:

$$\sigma=\sigma_0\exp\left[-\left(\frac{T_0}{T}\right)^{1/2}\right]. \tag{2B}$$

For the less aged samples, a deviation from this law is observed at high temperature, although this is not obvious from Fig. 5. This point is made clearer in Fig. 6 for sample $T0$.

Besides the expected decrease of the room-temperature conductivity, the most striking effect of the thermal treatment is the marked increase of the slopes of those curves, that is to say, of T_0. As shown in Fig. 7, T_0 shows a linear dependence with t_a for long aging times:

$$T_0\approx ct_a\,. \tag{3}$$

.

Thus for long enough aging times ($t_a>40$ h), Eq. (2B) becomes

$$\sigma(t_a,T)=\sigma_0\exp\left[-\left(\frac{ct_a}{T}\right)^{1/2}\right]. \tag{4}$$

It must be emphasized that this expression has exactly the same functional dependence with t_a as the expression (1) has, previously obtained for the kinetics of the conductivity evolution during thermal treatment. Furthermore, the numerical coefficients have about the same value when one extrapolates Eq. (4) for temperatures up to 120 °C. Taking $T=T_a=120$ °C in Eq. (4), one obtains $T_a/c=21\pm3$ h as compared to $\tau=17\pm3$ h derived from Eq. (1) in the case of $T_a=120$ °C. Thus it appears that the observed conductivity decrease during aging is entirely determined by the variation of T_0, the main parameter representative of the hopping mechanism.

The other remarkable result coming out of the experiments appears in Fig. 8. In this figure, the whole set of data has been plotted as a function of the unique reduced variable $(ct_a/T)^{1/2}$. One can see that all the experimental points remarkably merge into a single universal curve. Therefore, if it

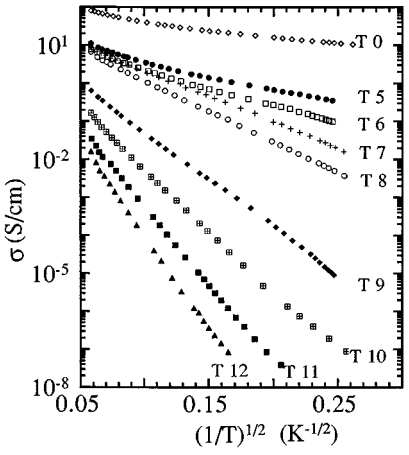

FIG. 5. Temperature dependence of the conductivity for PPY-ANS2 samples with various aging times.

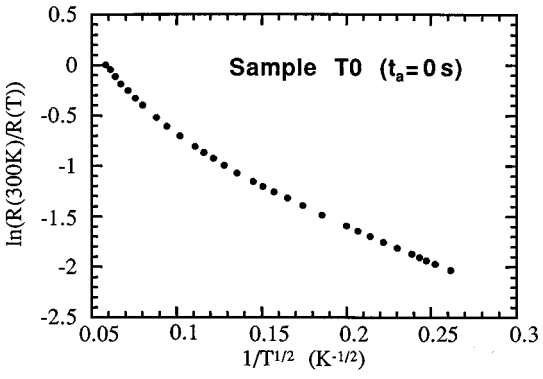

FIG. 6. Temperature dependence of the relative conductivity for the nonaged sample ($t_a=0$).

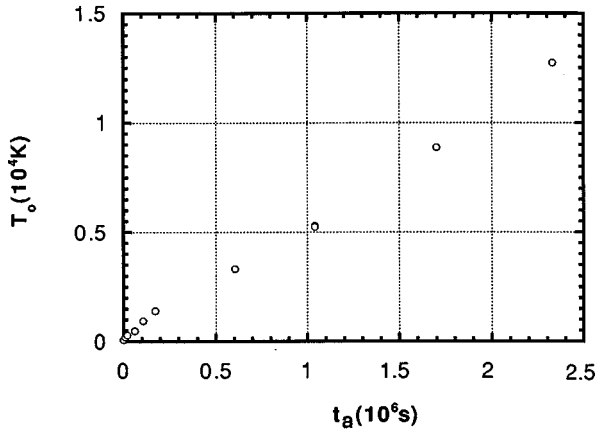

FIG. 7. Variation of the parameter T_0 derived from Eq. (2B) versus aging time t_a.

does exist, a power-law temperature dependence of the prefactor σ_0 should be of the form $(ct_a/T)^{\beta}$. Actually, the best numerical fits lead to the conclusion that β should be necessarily smaller than 0.5. As a first approximation, σ_0 can be considered as constant and neither temperature nor aging time dependent: $\sigma_0=20$ S/cm. In other words, the parameter T_0 is the only one relevant to describe the conductivity decrease and this leads to a remarkably simple expression of $\ln\sigma$ as a function of t_a and T:

$$\ln[\sigma(t_a,T)/\sigma_0]=-\left(\frac{ct_a}{T}\right)^{1/2}.$$

Such a hopping-type dependence cannot describe the conductivity of the highly conducting samples with aging time less than a few hours, i.e., samples $T0$, $T5$, and $T6$. A common feature of these samples is that the plot of $\ln(\sigma)$ versus $1/\sqrt{T}$ can be regarded as linear in the low-temperature range before deviating significantly at higher temperatures as shown in Fig. 6 for the reference sample $T0$.

As suggested in Refs. 2 and 19, an alternative way to determine the exponent α of the hopping law consists of calculating the reduced activation energy,

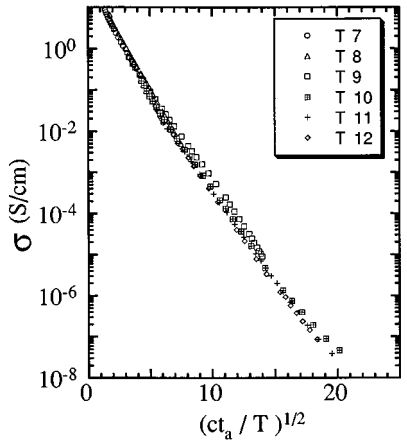

FIG. 8. Universal curve obtained by plotting the conductivity as a function of the reduced variable (ct_a/T) for samples with various aging times.

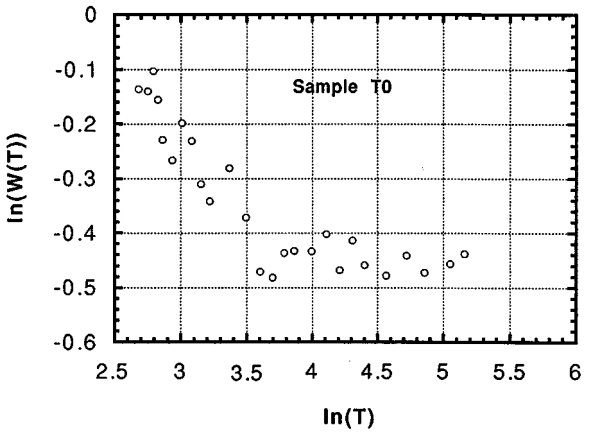

FIG. 9. Plot of ln(W(T)) versus ln(T) for the nonaged sample ($t_a=0$ s).

$$W(T)=T\,\frac{d\,\ln(\sigma(T))}{dT}.$$

From Eq. (2a), we obtain $\ln W(T)=A-\alpha\ln T$, where $A=\alpha\ln(T_0)+\ln(\alpha)$.

On the one hand, for the aged samples ($T11$, for instance, as shown in Fig. 9), the curve of $\ln(W)$ versus $\ln(T)$ is linear and the best fit leads to an estimated value for α of 0.47. On the other hand, for the nonaged sample we clearly obtain two distinct regimes (Fig. 10). The low-temperature data can be fitted with a straight line, the slope of which is about 0.45. This is in agreement with the fact that Eq. (2B) accounts well for the variation of σ in this temperature range. The high-temperature range with a lower value of α corresponds to a more slowly varying conductivity. Other models and transport mechanisms must be taken into account to explain the high-T regime. Typical crossover temperatures between the two regimes are 35 K for $t_a=0$ and 45 K for $t_a=900$ s.

In this respect, we have tried to fit our data with the fluctuation-induced tunneling (FIT) model of Sheng dedicated to the case of a parabolic insulating barrier[20] between large conducting grains. The conductivity is given by

$$\sigma=\sigma_0\exp\left(-\frac{T_1}{T+T_0}\right), \tag{5}$$

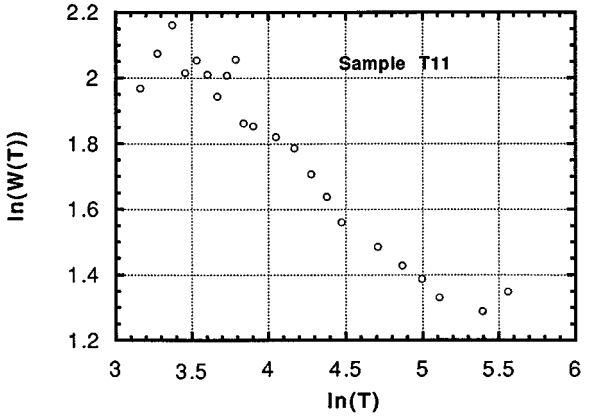

FIG. 10. Plot of ln(W(T)) versus ln(T) for the aged sample $T11$ ($t_a=1.7\times10^6$ s).

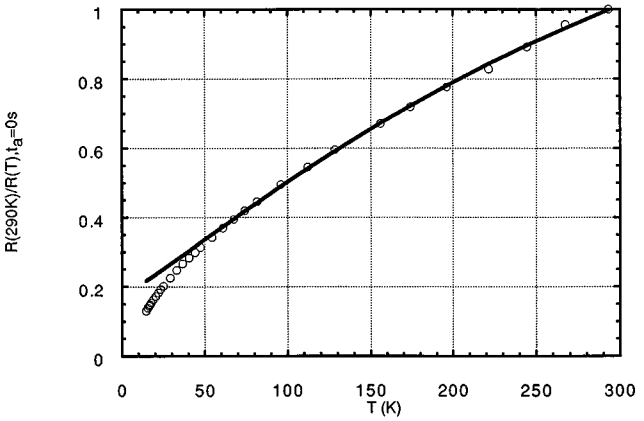

FIG. 11. Fit of the experimental data with the aid of the fluctuation-induced tunneling model [Eq. (6)] for the nonaged PPY/ANS2 sample ($t_a=0$ s). The parameters derived from the fit are $\sigma_0=2.36$, $T_0=375$ K, and $T_1=142$ K. The fit is valid above 50 K only.

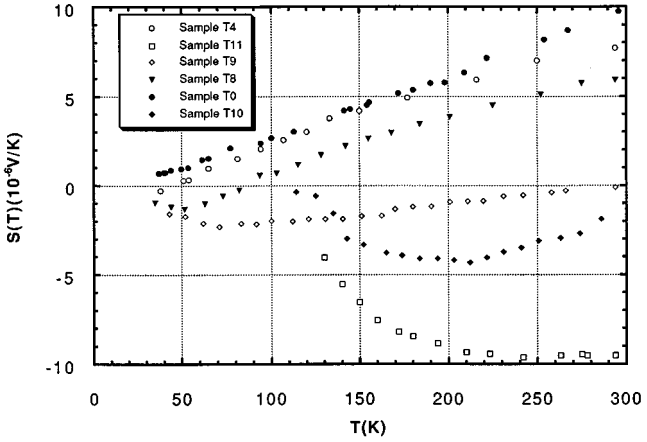

FIG. 12. Variation of the thermoelectric power as a function of temperature for the samples $T0$, $T4$, $T8$, $T9$, $T10$, and $T11$.

where σ_0, T_1, and T_0 are constants.

As shown in Fig. 11, for the nonaged sample, there is good agreement between the experimental data and the fit using Eq. (5) on a wide temperature range. A rather good agreement is also obtained for the sample with aging time $t_a=600$ s. Nevertheless, at low temperature, a discrepancy between the data and the FIT model appears. For the nonaged sample, the deviation starts at about 50 K. For the sample with aging time $t_a=600$ s, the crossover temperature is higher; the FIT model is valid in a narrower range and is less highlighted.

V. THERMOELECTRIC POWER VERSUS TEMPERATURE

The thermoelectric power of the material was measured by using a slowly varying, alternating temperature gradient method. The principle of the method was first discussed by Chaikin and Kwak.[21] The samples were mounted between two electrically isolated copper blocks placed upon a copper heat sink, and isolated from the latter. The copper blocks were glued with heaters. The temperature gradient between them never exceeded 0.5 K and was controlled with a Constantan/Cu thermocouple. A carbon-glass resistance together with a platinum resistance mounted in the heat sink were used to monitor the average assembly temperature. The output from the sample/Cu thermocouple was applied to the y axis of a recorder, and the output from the Constantan/Cu thermocouple was applied to the x axis of the recorder. Feeding the current alternatively to one or the other heater, the temperature gradient could be swept from negative to positive values. The resulting plot is a straight line, with a slope equal to the ratio of the thermoelectric power of the two thermocouples, sample/Cu over Constantan/Cu. The thermopower of copper, $S_{\mathrm{Cu}}(T)$, was taken as a linear function of

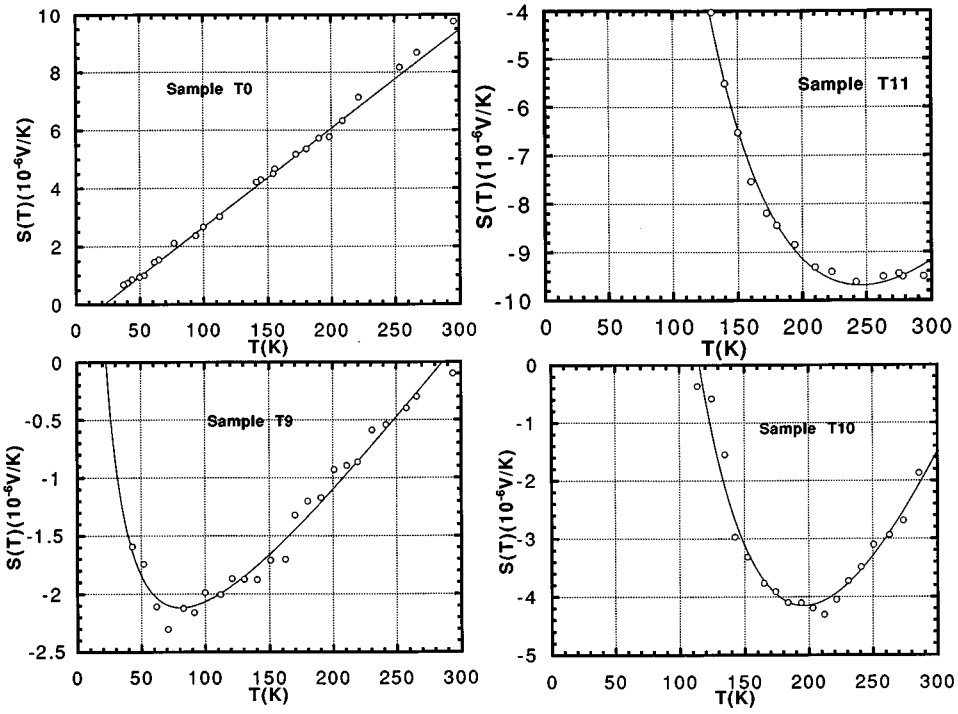

FIG. 13. Fits of the thermoelectric power data with $S(T)=AT+B+C/T$ for the samples $T0$, $T9$, $T10$, and $T11$. The fitting parameters are listed in Table II.

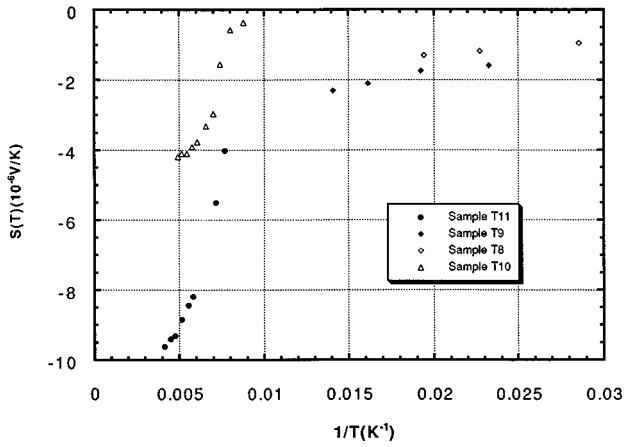

FIG. 14. Thermoelectric power versus $1/T$ for the samples $T8$, $T9$, $T10$, and $T11$. For clarity, only the points corresponding to temperatures below the minimum of the U-shaped curves of Fig. 12, where the C/T contribution is expected to prevail, have been plotted.

T with a room-temperature value of 1.6 μV/K. We were not able to extend the thermopower data to very low temperatures for the aged samples because of the difficulty to measure low voltages in high resistivity samples.

The thermoelectric power temperature dependences of samples $T0$, $T4$, $T8$, $T9$, $T10$, and $T11$ are shown in Fig. 12. We observe rather low thermopower values. For the unaged sample, a room-temperature value of 9.75 μV/K was measured. Room-temperature thermopower displayed a change of sign as a function of aging. The data obtained for samples $T0$ and $T4$ are well described on the whole temperature range with a linear law of the form $S(T)=AT+B$, which accounts for the fact that the thermopower does not extrapolate through the origin as can be seen in Figs. 12 and 13. At the early stage of the aging process, the thermopower data appear to be rather insensitive to the details of the temperature dependence of the resistivity and the slope of the $S(T)$ curves remains nearly constant. Our data are similar to results obtained from polypyrrole samples[22,23] and from a number of partially doped conducting polymers.[24–26]

For samples $T8$ to $T11$, the temperature range can be divided into two regions (Figs. 12–14). The high-temperature regime remains linear and no clear evolution of the slope with aging could be brought to the fore. In the low-temperature range, there is a clear deviation from linearity. Bender *et al.*[22] also found that thermally aged samples develop extra structures in their low-temperature thermopower. Moreover, the behavior is similar to the characteristic U-shaped dependence well known for HCl-doped polyaniline.[27] Such a dependence was also observed in PANI-CSA/PMMA (polyaniline camphor sulfonic acid/polymethylmethacrylate) blends near the percolation threshold.[28,29] The crossover temperature separating the two regions is an increasing function of the aging time. In the low-temperature range, the data can be fitted using the relation $S(T)=C/T+B$ as can be seen in Fig. 14 where the values of S obtained for samples $T8$ to $T11$ for temperatures below the minimum are plotted versus $1/T$. For the less aged samples, such a U-shaped dependence could not be observed but it may occur at lower temperatures where the high resistivity of the sample prevents any accurate thermoelectric power measurement. Therefore, the whole data set can be fitted using a sum of three contributions $S(T)=AT+B+C/T$ where A, B, and C are only weakly temperature dependent. The values of these parameters are listed in Table II and the results of the fittings are presented in Fig. 14.

VI. INTERPRETATION OF THE RESULTS IN TERMS OF CONDUCTING POLARONIC CLUSTERS

The conductivity evolution with aging time and temperature can be accounted for in the framework of two limiting conduction processes, standing for long and short aging times. However, a unified picture of the aging process will emerge. Let us first focus on aged samples.

A. Long aging times

1. dc conductivity

Several models lead to the functional dependence of the conductivity given by Eq. (2B). Let us now review and discuss the different models. According to the Mott variable-range hopping (VRH) model,[3] the transition rate p for hopping between localized centers is

$$p=p_0\exp(-2\gamma r)\exp(-\Delta E/kT),$$

where p_0 is a constant, r the distance between two sites, $1/\gamma$ the decay length of the localized wave function, and ΔE the activation energy for the hopping process. By maximizing p with respect to r, Mott then predicted the temperature dependence given by Eq. (2A), where α is determined by the dimensionality d of the carrier hopping: $\alpha=1/(d+1)$.

As a matter of fact, α would be equal to $\frac{1}{2}$ for one-dimensional transport. But in this model the preexponential factor should vary with temperature as $1/T$ in contradiction to experimental results in which σ_0 does not depend on temperature. Besides, it has been emphasized that extending Mott and Davis' arguments to 1D systems is not correct and that the conductivity follows a thermally activated law in the case of 1D VRH.[30,31]

Wang *et al.*[5] interpreted the $\alpha=\frac{1}{2}$ exponent by invoking a model of quasi-1D variable range hopping. For weak interchain coupling, only the nearest-neighboring chains are considered. The interchain hopping conductivity perpendicular to the chain is expressed as follows:

$$\sigma_\perp=\frac{2e^2g(Ef\ )b^2\nu_{\rm ph}(t_\perp\tau)^2}{A\hbar^2}\exp\left[-\left(\frac{T_0}{T}\right)^{1/2}\right],$$

where τ is the mean-free time, b the transverse localization length, A the average cross section of each chain, $g(E_F)$ the density of states at the Fermi level, $t_\perp$ the interchain transfer integral, $\nu_{\rm ph}$ a typical phonon attempt frequency (10^{13+} Hz), and

$$T_0=\frac{8\gamma}{g(E_F)k_B},$$

where γ is the inverse of the longitudinal localization length.

The interchain hopping conductivity parallel to the chain direction is given by

$$\sigma_{\parallel}=\frac{e^2\nu_{\mathrm{ph}}t_{\perp}^2\tau^2}{Azk_BT\hbar^2\gamma}\exp\left[-\left(\frac{T_0}{T}\right)^{1/2}\right],$$

where z is the number of nearest-neighboring chains. Due to the finite polymer length and occasional large interchain barriers, the interchain conductivity is expected to be much smaller than the intrachain one. It should determine the observed temperature dependence.

In this model, T_0 and the prefactor σ_0 are both functions of $g(E_F)$ and of the longitudinal localization length γ. Thus, σ_0 can be partly expressed as a function of T_0: $\sigma_0 \propto g(E_F)/T_0^2$ for the perpendicular interchain conductivity and $\sigma_0 \propto 1/\gamma T_0^2$ for the parallel one. Since, on one hand, T_0 is proportional to the aging time t_a and γ is expected to increase with aging and, on the other hand, $g(E_F)$ is more likely constant or possibly slightly decreasing, one should expect in both cases a two order of magnitude decrease for σ_0, which is in complete disagreement with the results.

A value of the exponent α equal to $\frac{1}{2}$ is also expected when the conduction mechanism is controlled by Coulomb interactions that create a gap in the density of states near the Fermi level as shown by Efros and Shklovskii.[4] The density of states tends towards zero as the square of the energy E referred to the Fermi level. In that case and in contrast with the two previous models, the prefactor is regarded as constant. However, some studies have pointed out that this model is relevant only at very low temperatures and that the conductivity is expected to exhibit a smooth crossover to the Mott behavior at higher temperatures ($\alpha=\frac{1}{4}$).[19,32] On the contrary, for aged samples, the temperature dependence of the conductivity is well fitted with $\alpha=\frac{1}{2}$ from 15 K up to room temperature. Moreover, in the framework of this model,[4] the localization length, which is proportional to $1/T_0$, would be decreased by two orders of magnitude upon aging. Such a huge variation is very unlikely to be of physical significance. The Efros-Shklovskii model can thus be ruled out.

To our knowledge, the last model leading to the former functional dependence was proposed by Zuppiroli *et al.*[8] It is based on the Sheng model of charging-energy-limited tunneling (CELT), originally proposed for granular metals in which conduction is supposed to proceed from tunneling between small conducting grains separated by insulating barriers.[6,7] Apart from the tunneling process, the number of charge carriers, which is controlled by the charging energy E_c, appears as a crucial parameter for the conductivity. E_c is nothing but the electrostatic energy required to create a positive-negative charged pair of grains. The basic assumption of the model is that E_c is large as compared to the thermal energy kT. Such a condition is all the more easily fulfilled as the grains are small. The major aspect introduced in the model by Zuppiroli *et al.* concerns, on one hand, the nature of the conducting state and, on the other hand, the origin and the characteristics of the grains clusters in the following, in strongly disordered conducting polymers. The conducting clusters are highly doped polaronic islands generated by heterogeneities in the doping distribution. The dopant ions act as tunneling bridges between neighboring chains and therefore improve the charge carrier motion. The prefactor σ_0 is considered as temperature independent in a first approximation.[33] As concerns the parameter T_0, it is given by

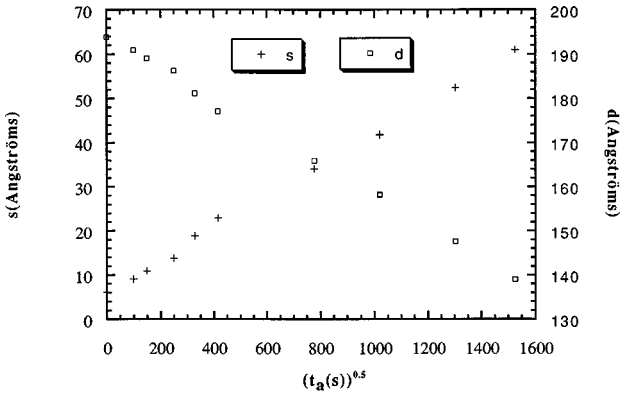

FIG. 15. Evolution of the conducting clusters' diameter d and of their separation s as a function of the square root of the aging time t_a. These values were derived from T_0, with the assumption $s+d=200$ Å. The parameter T_0 itself was deduced from the whole temperature range for long aging times ($t_a>10^5$ s) and from the low-temperature data for the short aging times ($t_a<10^5$ s) (see text). The vertical line separates the long- and short-aging-time regimes.

$$T_0=\frac{8U}{k_B}\frac{s^2}{d^2}\frac{1}{\frac{1}{2}+s/d}, \tag{6}$$

where d is the average diameter of the cluster, s the average distance between the clusters, and U the on-site Coulomb repulsion with an estimated value (from electron spin resonance measurements) of about 2 eV.[34,35]

We assumed that the Coulomb repulsion U remained constant as a function of aging. The x-ray photoemission spectroscopy measurements, especially the N($1s$) spectra, have indicated a slight dedoping with aging. One could thus expect a slight change in the on-site Coulomb repulsion U. Nethertheless, the parameter T_0 displays an increase of more than two orders of magnitude with aging. Such a huge variation cannot be ascribed to a change in U, that should remain around a few eV. Therefore, most of the T_0 evolution can be attributed to the geometrical characteristics s and d. At least in a first approximation, the assumption of a constant U is thus partially justified. d and s are related to the average distance between dopants ions, δ, and to the local average distance between dopants inside a cluster, δ, by the relation $\delta/\delta=d/(d+s)$. The charging energy is expressed as follows:

$$E_c=\frac{2Ua}{d(1+d/2s)}, \tag{7}$$

where a is the monomer size. In the following, we have taken $a=5$ Å. From the evolution of T_0, we have estimated the dependence of s and d with the aging time. We assumed $s+d$ constant and of the order of 200 Å, which appears to be, for example, the order of magnitude of the grain size in polyaniline as derived by Zuo *et al.*[36] This choice will be justified by the coherence of the model detailed in the following. In such a case, as illustrated in Fig. 15, the diameter d of the clusters decreases with increasing aging time, while the intergrain separation increases. In this picture, the conductivity decrease with aging results from a progressive degradation of the conducting islands. Therefore, the degradation mechanism would very likely be initiated at the grain

TABLE II. Parameters A, B, and C deduced from the fits $S(T)=AT+B+C/T$ for the samples $T0$, $T4$, $T8$, $T9$, $T10$, and $T11$.

Sample	$T0$	$T4$	$T8$	$T9$	$T10$	$T11$
B (μV/K)	0.74	1.05	4.16	4.45	33.1	35.7
A (μV/K^2)	3.410^{-2}	3.210^{-2}	4.110^{-2}	1.410^{-2}	7.410^{-2}	5.310^{-2}
C (μV)	<20	<20	52.5	94.7	2843	3189

surface, i.e., in the intergrain zone which is actually the defective zone. More precisely, for long aging times, the linear dependence of T_0 with aging time can be understood with a parabolic variation of s with the time $s \propto \sqrt{t_a}$. Such an increase of the distance between two conducting grains is similar to that observed for corrosion where the barrier separation is replaced by the thickness of the oxydized layer.[37]

In their work, Zuppiroli *et al.* paid particular attention to the basic questions concerning the multiphonon aspects of hopping. The electron lattice coupling constant g is nothing but the ratio of the polaron binding energy to the vibrational energy $\hbar w$ corresponding to the typical phonons involved in the hopping process. For a polaronic cluster with n monomers, it is $g=E_b/n\hbar w \approx 5/n$, where E_b is the lattice deformation energy. Taking the derived values for the cluster size leads to the conclusion that we are always in the weak-coupling limit. Therefore, the basic assumption of the model is fulfilled.

A similar functional form of the behavior of the conductivity change with the temperature has been observed in other conducting polymers, such as PANI and PANI derivatives.[38] Nevertheless, comprehensive analysis of the conductivity data in these various conducting polymers is needed to discriminate among the different conduction models.

2. Thermopower

The picture which we invoke to account for the conductivity evolution can be related to the thermoelectric power data in the framework of the Kaiser model for heterogeneous materials.[39] We will first briefly review the models relevant in homogeneous media.

A linear temperature dependence, $S(T)$, usually corresponds to the characteristic thermopower of a metal due to tunneling between states at E_F. This has already been observed in highly conducting polyacetylene.[24–26] For a disordered system, with a partially filled band there is a finite density of state at the Fermi energy. If the disorder is sufficiently weak that E_F lies in the energy range of extended states, the thermopower is expressed as follows:[3]

$$S=-\frac{k^2\pi^2}{3q}\,T\left|\frac{d\,\ln\sigma(E)}{dE}\right|_{E_F}, \tag{8}$$

where k is the Boltzman constant, q is the charge of the carrier, E_F is the Fermi energy, and the energy dependence of the conductivity, $\sigma(E)$, generally arises from both the band structure and the energy dependence of the scattering time.

The positive sign of the slopes of the $S(T)$ curves in the high-temperature limit indicates that the dominant conduction mechanism takes place above the Fermi level. Thus, the experimental linear contribution to the thermoelectric power should very likely proceed from the highly conducting clusters.

In amorphous semiconductors, in which hopping between band tail localized states dominates the transport process, the thermoelectric power can be written[3,40] as

$$S(T)=B+C/T, \tag{9}$$

where B and C are determined by the energy distribution of the density of localized states and by the nature of the scattering process. Moreover, if E_g is the energy gap at the Fermi energy, one gets $B \approx E_g/e$. From the data, we derive $E_g=0.05$ meV for $T8$ and $E_g=3.2$ meV for $T11$. These values seem too small for the model to be consistent since $E_g \gg kT$ is required. Nethertheless, as explained further, it should be pointed out that the heterogeneous structure of the material leads to additional prefactors preventing an accurate estimation of the gap. Such a contribution should be characteristic of the insulating barrier separating the polaronic clusters.

At this point, let us now review the predictions of the other conduction models previously discussed, as concerns the thermopower behavior. In the case of the Efros-Shklovskii transport model, S is expected to be constant.[41] Several models for the thermoelectric power behavior have been proposed in the case of the variable-range hopping transport mechanism. It appears that S varies as $T^{1/2}$, $T^{3/4}$, or $T_0^{1/4}T^{3/4}+T$ in three dimensions.[3,41,42] None of these models can actually account for our data especially in the low-temperature range, where variable-range hopping, if ever it occurs, is expected to prevail.

In quasi-1D VRH,[27] $S(T)$ is given by

$$S(T)=\frac{k}{2e}\,\frac{W^2}{kT}\left|\frac{d\,\ln f(E)g(E)\mu(E)}{dE}\right|,$$

where W is the range of energy contributing to conduction, f is the Fermi distribution function, μ is the mobility, and g the density of states. According to Mott and Davis, W is assumed to be the hopping energy. For the interchain hopping in quasi-1D VRH, $W \propto k(T_0T)^{1/2}$ and thus $S \propto T_0$. For the intrachain hopping, one has $W \propto kT_0$ and therefore $S \propto T_0^2/T$. The total thermopower in quasi-1D VRH is contributed by both interchain and intrachain hopping, so that the expected T dependence is of the form $B+C/T$. Nevertheless, in the framework of this model, B and C should be of the same sign which is experimentally never the case as can be seen in Table II. Moreover, it can be easily shown that for samples $T8$, $T9$, $T10$, and $T11$ the ratio C/B is not a linear function of T_0 deduced from the conductivity data contrary to what is expected in this model. Sample $T8$, the conductivity of which follows the (2B) law on the full temperature range,

exhibits a linear thermopower on a wide temperature range, suggesting that metallic islands cannot be ignored in the conduction process and that the $\frac{1}{2}$ exponent is the result of the granular structure of our very disordered material and not of a quasi-one-dimensional VRH process.

As strongly suggested by the conductivity measurements, our samples display a granular structure. Therefore, the total thermoelectric power should be the superposition of the two contributions corresponding to the conducting grains and to the insulating barriers. For a heterogeneous material, made up of metallic and amorphous semiconductinglike regions, one has to take into account the nonlinearities of the temperature gradient due to the different thermal resistances W_m and W_{sc} of each region. In the very simple case where the two types of region are in series along the thermal gradient, the thermopower can be expressed as the sum of two parts,[39]

$$S=\frac{\Delta T_m}{\Delta T}S_m+\frac{\Delta T_{sc}}{\Delta T}S_{sc}$$

or using the proportionality between the thermal resistance and the temperature gradient

$$S(T)=\frac{W_m}{W}S_m+\frac{W_{sc}}{W}S_{sc},$$

where W and ΔT are the total thermal resistance and temperature gradient, respectively, ΔT_m and ΔT_{sc} are the sum of the temperature drops in the metallic and the amorphous semiconducting regions, and S_m and S_{sc} their intrinsic thermoelectric powers. Replacing S_m and S_{sc} by their values from Eqs. (8) and (9) leads to a functional dependence with three contributions, $S(T)=AT+B+C/T$. Therefore, the changes observed in the ratios B/A and C/A, as deduced from the fittings of $S(T)=AT+B+C/T$ on the experimental data, should reflect a possible evolution of the microscopic parameters included in the thermoelectric powers S_m or S_{sc}, like $|d\ \ln \sigma(E)/dE|_{E_F}$ or E_g, but also the variation of the relative proportion of the two phases through the ratio W_{sc}/W_m. Thus, B/A and C/A are expected to increase with aging, together with the size of the amorphous semiconducting region.

In a very simplified way, B/A and C/A can be related to s and d, the relevant lengths for the semiconducting and metallic regions, and to their thermal resistivities ρ_m and ρ_{sc} by

$$\frac{B}{A}\frac{C}{A}\propto\frac{W_{sc}}{W_m}\propto\frac{\rho_{sc}}{\rho_m}\frac{s}{d}.$$

The experimental variation of B/A and C/A are reported in Fig. 16 as a function of the aging time. They are both increasing and nearly linear functions of t_a and display a striking similarity with the behavior of s/d as deduced from T_0. Actually, from Eq. (6), one can derive in a first approximation that $s/d\propto T_0\propto t_a$ for long aging times.

The precise relationship between B/A, C/A, and s/d is certainly more complex but it can be deduced from the former discussion that the analysis of the thermopower data strongly supports the idea that the metallic cluster size undergoes a clear decrease with aging. To give additional support to our picture, it must be pointed out that a similar U-shaped dependence was observed in PANI-CSA/PMMA

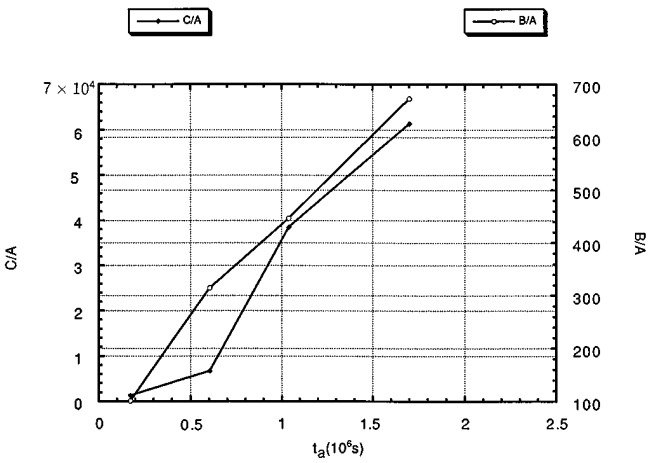

FIG. 16. Plot of B/A and C/A versus the aging time t_a.

blends near the percolation threshold.[28,29] As the blends are diluted, the temperature dependence remains linear at high temperature, but shows a clear deviation below 100 K. It was also attributed to activated transport between disconnected regions, large scale inhomogeneities, and highly conducting islands separated by insulating regions. Therefore, one can speak of a certain analogy between our material and the PANI-CSA/PMMA blends. On the one hand, the highly conducting islands in the polypyrrole samples correspond to the highly conducting PANI regions in the blends and lead to the linear term in the thermoelectric power. On the other hand, the less conducting regions separating the conducting clusters in polypyrrole correspond to the insulating matrix of PMMA and are related to the semiconductinglike contributions in the thermoelectric power.

At this point, we are dealing with a representation of both the conduction mechanism and the aging process, which remarkably accounts for the temperature and time evolution of the conductivity and the temperature dependence of the thermopower, at long aging times. It is therefore tempting to consider the case of short aging times starting from the framework of this picture. The extrapolation of the variation of s and d leads to larger clusters at short aging times. Given the fact that the charging energy E_c is a decreasing function of the grain size, one expects E_c to be smaller and smaller when going to shorter and shorter aging times. Since E_c is of the order of the thermal energy at room temperature for sample $T7$ ($t_a=10^5$ s) (see Table III and the next section), it

TABLE III. Grain size, intergrain distances, and E_c orders of magnitude derived from T_0 [Eq. (6)] for the sample $T0$ ($t_a=0$ s) and for a long-aging-time sample $T7$ ($t_a=1.7\times10^5$ s) supposing that $d+s=200$ Å. At room temperature, $k_BT=2.58\times10^{-2}$ eV.

	Sample $T0$	Sample $T7$
t_a (s)	0	10^5
T_0 (K)	90	938
s/d	0.016	0.054
s (Å)	3	11
d (Å)	200	190
E_c (eV)	3×10^{-3}	1×10^{-2}

TABLE IV. Cross-over temperatures above (FIT) or below (Zuppiroli) which the discrepancy between the best fits based on Eq. (5) or Eq. (2B) and the experimental data are within a maximum of ten percent. Tc is the theoretical transition temperature between the two distinct transport mechanisms (see text).

t_a (s)	0	900
Crossover temperature for the Zuppiroli fit [Eq. (2B)]	$T<54$ K	$T<88$ K
Crossover temperature for the Sheng fit [Eq. (5)]	$T>16.5$ K	$T>24$ K
$T_c(E_c=k_BT_c)$	35 K	44 K

is clear that the CELT between conducting clusters can only be valid at lower and lower temperatures when going from samples $T7$ to $T0$. In agreement with our previous analysis, another model must be invoked in these samples for temperatures higher than a crossover temperature T_c equal to about E_c/k. This point will be discussed in the next section.

B. Short aging times

The charging energy E_c has been derived for the various samples from Eq. (7). In the case of short-aging-time samples, T_0 was estimated from the slope of the $\ln(\sigma)$ versus $1/\sqrt{T}$ plot in the low-temperature range. Then d/s, d, s, and finally E_c were deduced using the previous assumption, i.e., $d+s\approx 200$ Å. The results are summarized in Table III and Fig. 15 with those obtained for long aging times.

Using the relation $E_c=kT_c$, we have estimated the transition temperature T_c, for a given E_c, above which the model does not apply. The results are listed in Table IV. The values are actually in good agreement with those previously obtained from the plot of $\ln W(T)$ versus $\ln(T)$ (see Sec. I). Thus, in less aged samples ($T0,\ldots,T6$), we are dealing with large clusters separated by insulating barriers. It is therefore quite natural to invoke the FIT model proposed by Sheng.[20] In this model, the system is made up of large conducting regions separated by thin insulating barriers. The voltage across these barriers is subject to large thermal fluctuations, leading to a modulation of the tunneling probability and introducing a characteristic temperature dependence of the conductivity. Assuming parabolic barriers described by two parameters T_1 and T_0, the conductivity is expressed by Eq. (5). As a matter of fact, there is rather good agreement with the experimental data as shown in Sec. I.

For both the nonaged ($T0$) and the 600-s aging time sample ($T1$) we have performed a double theoretical fit. At high temperature, using the FIT behavior (Eq. 6), we determined the temperature below which the deviation between the data and the theoretical law was larger than 10%. On the opposite, using the hopping behavior [Eq. (2b)] at low temperatures, we determined the temperature above which the same deviation was larger than 10%, too. The results are presented in Table IV. The good agreement and the coherence between these independent estimates of the crossover temperature gives an argument in favor of the conducting islands approach.

Let us now compare the physical parameters deduced from the fluctuation-induced tunneling model with those derived from the Zuppiroli model. With this aim, we used the phenomenological relationships between T_0, T_1, and the barrier parameters, proposed by Schimmel.[43] The height of the barrier is given by

$$\Delta E=k_BT_1, \tag{10}$$

while its width s is related to T_0 and T_1 by

$$\frac{T_1}{T_0}=\sqrt{2m\Delta E}\,\frac{2s}{\hbar}. \tag{11}$$

TABLE V. Barrier parameters derived from the phenomenological model of Schimmel [Eqs. (10) and (11)] for sample $T0$ ($t_a=0$ s). The data points were fitted on the whole temperature range or above 100 K.

Limiting fit temperature (K)	$T>15$ K	$T>100$ K
s (Å)	26	10
ΔE (eV)	1.79×10^{-2}	4.8×10^{-2}

Orders of magnitude of ΔE and s derived from T_0 and T_1 are given in Table V for the samples with aging time $t_a=0$ and $t_a=600$ s. The numerical estimates of the barrier width in general do not differ much from our estimated values.[25,43] Moreover, they are consistent with the independent determination obtained from the conducting cluster model. Yet, there remains a slight deviation between the two determinations for s. This discrepancy may have several origins: (i) The FIT model reduces the general behavior of a whole set of different junctions to the one of a single junction with appropriate values of T_1 and T_0. Therefore, the calculated parameters represent only an order of magnitude of the average characteristics of the barriers; (ii) the imprecise determination of the parameter T_1 and T_0 due to a limited fitting temperature range. The complete application of the fluctuation-induced tunneling model[44] leads to barrier widths of the same order of magnitude.

Finally, we attempted to correlate the temperature dependence of the conductivity for the less aged samples with the short time decay of σ during aging and to explain the deviation observed on the beginning of the kinetics curve of Fig. 2. Starting from the FIT law Eq. (5), and assuming that s is the only junction parameter which varies with the elapsed time, and that the height of the barrier remains constant, leads to an expression of σ as a function of the single variable s. At the aging temperature T_a, the following relation is then obtained:

$$\sigma=\sigma_0\exp\left(-\frac{2\sqrt{2}\Delta Es(t_a)\sqrt{m\Delta E}}{(2\sqrt{2}T_aks(t_a)\sqrt{m\Delta E}+\Delta Eh)}\right).$$

Developing this expression around the value of s at the beginning of the thermal treatment, under the assumption $\Delta\sigma/\sigma\leqslant 1$, leads to the following relation: $\Delta\sigma/\sigma\propto\Delta s$. Again, a metal-like corrosion mechanism with a parabolic variation of the thickness of the oxidized material versus time (Δs proportional to $\sqrt{t_a}$) appears to be consistent with the conductivity degradation of the samples experimentally observed at its early stage ($\Delta\sigma/\sigma\propto\sqrt{t_a}$).

At this point it is interesting to compare the present work with the work by Reghu and co-workers.[1,2] Reghu and coworkers are dealing with PANI/CSA samples near the metal-insulator transition in which, in a very simplified way, a scaling temperature dependence of the conductivity is changed to a variable-range-hopping law when the aging time increases on the insulating side of the transition. We are here concerned with polypyrroles far from this transition, in which the fluctuation-induced tunneling temperature dependence of the conductivity is replaced by charging-energy-limited tunneling between clusters. Nevertheless, the transport process which prevails in the aged samples considered by Reghu and co-workers seems not to correspond to the one in our pristine materials. As a matter of fact, in the case of the PANI/CSA samples, the localized states seem to be homogeneously distributed inside the material during aging and therefore no well-defined conducting clusters seem to be created. On the contrary, in our polypyrrole samples the granular structure precedes any structural or chemical changes through aging. In that case, the material is characterized by a heterogeneous structure at the very beginning of the aging process.

VII. CONCLUSION

In the present work, the effects of aging on the electronic conduction mechanism of polypyrrole were studied by combining the time dependence of the dc conductivity during aging at a given temperature and the temperature dependence of both the conductivity and the thermoelectric power for different aging times. Concerning the temperature dependence of σ, two distinct and characteristic transport mechanisms have been identified that depend on the increasing disorder produced by thermal degradation. For the more aged samples, the prevailing conduction mechanism is charging-energy-limited tunneling between polaronic clusters. The conducting grain size was estimated to be about 200 Å. The intergrain separation increases from 3 to 30 Å after 1-month aging at 120 °C. For the less aged samples, the high-temperature regime of the conductivity is characteristic of the fluctuation-induced tunneling mechanism between large grains. The samples with intermediate aging exhibit a crossover from one transport process to another with a threshold characteristic of the charging energy and thus of the size of the highly conducting islands. The thermopower measurements demonstrate clearly the heterogeneous structure of the material and the decreasing contribution of conducting regions to the electronic transport properties upon aging. They give strong support to the picture deduced from the conductivity data.

Concerning the aging time dependence of the conductivity, a parabolic relative decay was observed for short thermal treatment times as already observed on several conducting polymers. Yet, we pointed out a crossover towards a nontrivial stretched exponential behavior for long aging times. We have shown that this crossover is consistent with the change of the transport mechanism. The parameter T_0 of the conducting law entirely determines the degradation kinetics and a single expression can account for both the temperature and aging time dependence of σ for the aged samples:

$$\ln\sigma(t_a,T) \propto -\left(\frac{t_a}{T}\right)^{1/2}.$$

The key factor affecting the conductivity decay with aging seems to be the decreasing conducting grain size caused by oxidization with a kinetic similar to those encountered in corrosion mechanisms, since a parabolic variation of s with aging time gives a suitable description of the two regimes. Nevertheless, the details of such a degradation process are not yet understood but, considering the expected complexity and variety of chemical changes in the material (loss of structural water, oxidization of the polymer backbone, defects on the doping centers), the continuity in the evolution of the conductivity with the single law $\sigma=\sigma_0\exp(-\sqrt{t_a/\tau})$ suggests that some slow process is the limiting step for the various reactions leading to the formation of the defects.

ACKNOWLEDGMENT

One of us (J.P.T.) would like to acknowledge A. Moliton for several suggestions about the study of conduction mechanisms in conducting polymers.

[1] M. Reghu, C. O. Yoon, D. Moses, A. J. Heeger, and Y. Cao, Phys. Rev. B **48**, 17 685 (1993).
[2] C. O. Yoon, M. Reghu, D. Moses, and A. J. Heeger, Phys. Rev. B **49**, 10 851 (1994).
[3] N. F. Mott and E. A. Davis, *Electronic Processes in Non-Crystalline Materials*, 2nd ed. (Clarendon, Oxford, 1979).
[4] A. L. Efros and B. J. Shklovskii, J. Phys. C **8**, L49 (1975).
[5] Z. H. Wang, A. Ray, A. G. MacDiarmid, and A. J. Epstein, Phys. Rev. B **43**, 4373 (1991).
[6] P. Sheng, B. Abeles, and Y. Arie, Phys. Rev. Lett. **31**, 44 (1973).
[7] B. Abeles, P. Sheng, M. D. Coutts, and Y. Arie, Adv. Phys. **24**, 407 (1975).
[8] L. Zuppiroli, M. N. Bussac, S. Paschen, O. Chauvet, and L. Forro, Phys. Rev. B **50**, 5196 (1994).
[9] R. H. Baughman and L. W. Sacklette, Phys. Rev. B **39**, 5872 (1989).
[10] J. C. Thieblemont, M. F. Planche, C. Petrescu, J. M. Bouvier, and G. Bidan, Synth. Met. **59A**, 81 (1993).
[11] V. T. Truong, Synth. Met. **52**, 33 (1992).
[12] V. T. Truong, B. C. Ennis, T. G. Turner, and C. J. Jenden, Polymer **27**, 187 (1992).
[13] H. Münstedt, Polymer **29**, 296 (1988).
[14] T. L. Tansley and D. S. Maddison, J. Appl. Phys. **69**, 7711 (1991).
[15] L. A. Samuelson and M. A. Druy, Macromolecules **19**, 824 (1986).
[16] B. Sixou, N. Mermilliod, and J. P. Travers, Europhys. Lett. **30**, 157 (1995).
[17] R. L. Elsenbaumer, C. Maleysson, and K. Y. Jen, Polym. Mater. Sci. Eng. **56**, 54 (1987).
[18] T. Ishiguro, H. Kaneko, Y. Nogami, H. Ishimoto, H. Nishiyama, J. Tsukamoto, A. Takahashi, M. Yamaura, and K. Sato, Phys. Rev. Lett. **69**, 660 (1992).

[19] C. O. Yoon, M. Reghu, D. Moses, A. J. Heeger, and Y. Cao, Synth. Met. **63**, 47 (1994).
[20] P. Sheng, Phys. Rev. B **21**, 2180 (1980).
[21] P. M. Chaikin and J. F. Kwak, Rev. Sci. Instrum. **46**, 218 (1975).
[22] K. Bender, E. Gogu, I. Hening, D. Schweitzer, and H. Müenstedt, Synth. Met. **18**, 85 (1987).
[23] D. S. Maddison, J. Unsworth, and R. B. Roberts, Synth. Met. **26**, 99 (1988).
[24] Y. W. Park, W. K. Han, C. H. Choi, and H. Shirakawa, Phys. Rev. B **30**, 5847 (1984).
[25] W. Pukacki, R. Zuzok, S. Roth, and W. Göpel, in *Electronic Properties of Polymers*, edited by H. Kuzmany, M. Mehring, and S. Roth, Vol. 107 of Springer Series in Solid-State Science (Springer, Berlin, 1992).
[26] H. H. Javadi, A. Chakraborty, C. Li, N. Theophilou, D. B. Swanson, A. G. MacDiarmid, and A. J. Epstein, Phys. Rev. B **43**, 2183 (1991).
[27] Z. H. Wang, E. M. Scherr, A. G. MacDiarmid, and A. J. Epstein, Phys. Rev. B **45**, 4190 (1992).
[28] C. O. Yoon, M. Reghu, D. Moses, A. J. Heeger, and Y. Cao, Phys. Rev. B **48**, 14 080 (1993).
[29] C. O. Yoon, M. Reghu, D. Moses, A. J. Heeger, and Y. Cao, Synth. Met. **63**, 47 (1994).
[30] Kurkijärvi, Phys. Rev. B **8**, 922 (1973).
[31] S. Alexander and R. Orbach, Physica B+C **107B**, 675 (1981).
[32] A. Aharony, Y. Zhang, and M. P. Sarachik, Phys. Rev. Lett. **26**, 3800 (1992).
[33] L. Zuppiroli (private communication).
[34] O. Chauvet, S. Paschen, L. Forro, L. Zuppiroli, P. Bujard, K. Kai, and W. Wernet, Synth. Met. **63**, 115 (1994).
[35] M. N. Bussac and L. Zuppiroli, Phys. Rev. B **49**, 5876 (1994).
[36] F. Zuo, M. Angelopoulos, A. G. MacDiarmid, and A. J. Epstein, Phys. Rev. B **36**, 3475 (1987).
[37] J. Besson, in *Corrosion des Matériaux à Haute Température*, edited by G. Beranger, J. C. Colson, and F. Dabsi (Les Editions de Physique, Paris, 1987).
[38] J. P. Pouget, S. L. Zhao, H. Wang, Z. Oblakowski, A. J. Epstein, S. K. Manohar, J. M. Wiesinger, A. G. MacDiarmid, and C. H. Hsu, Synth. Met. **55-57**, 341 (1993); F. Lux, G. Hinrichsen, V. I. Krinichnyi, I. B. Nazarova, S. D. Cheremisow, and M. M. Pohl, *ibid.* **55-57**, 347 (1993).
[39] A. B. Kaiser, Phys. Rev. B **40**, 2806 (1989).
[40] P. Nagels, in *Amorphous Semiconductors*, edited by M. H. Brodsky (Springer-Verlag, Berlin, 1985), Chap. 5.
[41] I. P. Zvyagin, Phys. Status Solidi B **58**, 443 (1973).
[42] P. Kuivalainen, H. Isotalo, and H. Stubb, Phys. Status Solidi B **122**, 791 (1984).
[43] Th. Schimmel, G. Denninger, W. Reiss, J. Voit, M. Schoerer, W. Schoepe, and H. Naarman, Synth. Met. **28**, 11 (1989).
[44] G. Paasch, G. Lehmann, and L. Wuckel, Synth. Met. **37**, 23 (1990).